Stable and selective dehydrocondensation of methane towards benzene on modified Mo/HMCM-22 catalyst by the dealumination treatment

Yuying Shu *, Ryuichiro Ohnishi, and Masaru Ichikawa †

Catalysis Research Center, Hokkaido University, Kita-Ku, N-11, W-10, Sapporo 060-0811, Japan

Received 20 November 2001; accepted 10 January 2002

A modified Mo/HMCM-22 catalyst by the dealumination treatment (Mo/HMCM-22-D) exhibited remarkable performance for the catalytic dehydrocondensation of methane with a higher selectivity of benzene and a lower selectivity of coke, in comparison with the same Mo catalyst supported on parent HMCM-22 (Mo/HMCM-22). Excellent catalytic stability as well as a high benzene formation rate of 1500 nmol/(g-cat·s) was obtained on a 6%Mo/HMCM-22-D catalyst at 1023 K, 3 atm and 2700 ml/(g·h) owing to the efficient suppression of coke formation. Dealumination of the HMCM-22 zeolite was characterized by XRD, ^{27}Al and ^{1}H MAS NMR and NH_3-TPD techniques. It was found that the dealumination treatment of HMCM-22 zeolite resulted in an effective suppression of acid sites, particularly the Brønsted acid sites (proton form in Al–O–Si) owing to the removal of tetrahedral framework aluminum, while the microporous structure and the zeolite framework remained unchanged. It was suggested that the stable and selective dehydrocondensation of methane towards benzene is based on the suppression of coke formation owing to the effective decrease of strong Brønsted acid sites by the dealumination treatment of the HMCM-22 zeolite.

KEY WORDS: methane; dehydrocondensation; benzene; dealumination treatment; HMCM-22; Mo catalyst; MAS NMR; NH_3-TPD.

1. Introduction

The conversion of methane to useful chemical products remains an important challenge and was a hot topic in the 20th century, especially in those days after the petroleum crisis [1]. During the past eight years, the direct conversion of methane to aromatics such as benzene and naphthalene, together with a considerable amount of hydrogen, was widely studied in terms of catalyst preparation, characterization and reaction mechanism [2–14]. Many researchers tested a lot of catalysts in order to improve the catalyst activity and selectivity, and the main literature results are summarized in table 1, which shows that Mo- and Re-supported HZSM-5 catalysts exhibited the highest catalytic performance in producing aromatics such as benzene and naphthalene [3–12]. Lunsford and co-workers [8,9] and Ichikawa and co-workers [10,11] have proceeded with a quantitative on-line GC analysis by using the internal standard method to make a mass balance of the product formation with the evaluation of the coke formation. Meanwhile, Solymosi *et al.* [6,7] and Lunsford and co-workers [8,9] suggested that there is an induction period during which the MoO_3 is reduced by methane to form Mo_2C, which in turn is responsible for methane activation. Ichikawa and co-workers [11] confirmed the formation of Mo_2C by means of the EXAFS technique coupled with TG-DTA-MASS. Recently, Borry *et al.* [13] have demonstrated the formation of an $(Mo_2O_5)^{2+}$ species on Mo/HZSM-5 during the exchange process. They have further traced its reduction and carburization in methane to form the MoC_x particles, as well as the concurrent regeneration of the bridging OH groups initially displaced by the Mo oxo dimers [14].

Most researchers believe that methane dehydrocondensation is a kind of bi-functional catalysis, both the transition metal and the zeolite support being essential components [2]. Concerning the zeolite support, some inspiring attempts have been made [11,15–18]. Recently, it has been reported that HMCM-22 zeolite is a good support and Mo/HMCM-22 is a selective catalyst for methane dehydroaromatization [17,18]. However, its catalytic activity still decreases with time on stream due to serious coke deposition on the catalyst surface. Therefore, it is of significance to develop useful methods for suppressing coke formation and improving catalyst stability. Efficient ways such as the adding of CO and/or CO_2 [19–21] into the methane feed and the steaming treatment of HZSM-5 zeolite [22] have been previously reported. On the other hand, it has been reported that the coke formation deposited on the Mo/HZSM-5 catalyst surface in methane dehydrocondensation is strongly affected by the strength and amount of zeolite acidity [11,22]. Accordingly, we studied the variation of HMCM-22 acidity with and without the dealumination

* On leave from the State Key Laboratory of Catalysis, Dalian Institute of Chemical Physics, China.
† To whom correspondence should be addressed.
E-mail: michi@cat.hokudai.ac.jp

1011-372X/02/0700-0009/0

Table 1
Literature survey of methane dehydrocondensation reaction over transition metal ion-loaded catalysts using various supports

Samples	Temperature (K)	Conversion of CH_4 (%)	Formation rate of aromatics (nmol/g·s)	Selectivity (%)				Ref.
				C_2	Benzene	Naphthalene	Coke	
Mo/HZSM-5	973	7.2	–	–	100 [a]	–	–	3
Zn/HZSM-5	973	1.0	–	–	79.1 [b]	–	–	4
Cu/HZSM-5	973	0.6	–	–	52.5 [b]	–	–	4
2Mo/HZSM-5	973	6.7	–	–	80.8 [b]	–	–	5
MoO_3/SiOux	973	5.4	3.31 [c]	–	–	–	–	6
MoO_3/Al_2O_3	973	0.23	0 [c]	–	–	–	–	6
K_2MoO_4/HZSM-5	973	5.2	14.0 [c]	–	–	–	–	7
MoO_3/HZSM-5	973	5.8	35.0 [c]	–	–	–	–	7
2Mo/HZSM-5	973	8.0	–	–	65.0	–	–	8
2Mo/HZSM-5	1023	7.6	15.4	–	–	–	–	9
2Fe/HZSM-5	1023	4.1	3.7	–	–	–	–	9
3Mo/HZSM-5	973	9.4	–	2.8	40.9	16.9	36.1	10
3Mo/USY	973	6.4	–	2.2	10.5	0	84.3	11
6Mo/H-β	973	6.7	–	3.6	14.2	2.5	71.5	11
5Re/HZSM-5	973	6.4	–	4.0	44.0	14.0	34.0	12
5Re/HZSM-5	1023	9.3	–	4.0	42.0	10.0	42.0	12

Carbonaceous deposits were neglected. Others were measured using an internal standard analyzing method basing on total carbon mass.
[a] Detected by FID.
[b] Detected by TCD.
[c] Calculated on the basis of H_2 and H_2O balance.

treatment and its effect on methane dehydrocondensation reaction. The dealumination treatment of HMCM-22 zeolite was conducted using the acid reflux method, according to the procedure reported in ref. [23]. Then the catalytic performance of Mo-supported HMCM-22 catalysts before and after the dealumination treatment for methane dehydrocondensation was studied. High-resolution solid-state ^{27}Al and ^{1}H MAS NMR, as well as NH_3-TPD techniques, were used to elucidate the variation of framework Al and acidity in the dealumination process.

2. Experimental

2.1. Catalyst preparation

The MCM-22 zeolite was synthesized using hexamethylenimine as a template according to the procedure described in the patent [24]. Briefly, certain amounts of sodium meta-aluminate, sodium hydroxide (96% NaOH), R (containing ~85% HMI), silica (95% SiO_2) and deionized water were added into a vessel under vigorous stirring for 30 min. The resulting gel was then introduced into a stainless steel autoclave and heated to 423 K for a certain time, until the gel crystallized completely. The as-synthesized sample was centrifuged at 5000 rpm, then washed and dried at 383 K overnight. The sample was then calcined in air at 810 K for 24 h to remove the template and yield the MCM-22 zeolite. The acid form of MCM-22 zeolite was obtained after successive exchanging with 1 mol/l NH_4NO_3 three times, then washed and dried. The following dealumination treatment of HMCM-22 zeolite was performed by acid reflux with an aqueous 6 M HNO_3 solution at 373 K for 10 h, as described in ref. [23]. It should be mentioned that, before the acid reflux treatment, HMCM-22 zeolite was calcined at 973 K in air for 10 h, in order to carry out the dealumination treatment more efficiently [23]. Consequently, the Si/Al atomic ratio increased to 19 from the initial value of 15, as determined by an XRF-1700 X-ray fluorescence spectroscope.

The loading of Mo (6 wt%) on the initial and dealuminated HMCM-22 was conducted by impregnating the zeolites with an aqueous solution of ammonium heptamolybdate (Kanto Chem. Co. of Japan, analytical grade) and denoted as 6%Mo/HMCM-22 and 6%Mo/HMCM-22-D, respectively. The samples were first dried at 343 K, and then heated up to 393 K and finally calcined at 773 K for 5 h, as described in previous studies [16–18].

2.2. Catalytic reaction

The reaction was carried out in a fixed-bed continuous-flow system at 973–1073 K and 3 atm, with a methane flow rate of 15 ml/min, and either in the absence or presence of CO_2. Briefly, 0.3 g of the catalyst was charged into a 6 mm i.d. quartz tubular reactor. The catalyst was first heated under an He stream (15 ml/min) to 873 K and maintained at this temperature for 30 min. Then a 10% Ar/CH_4 gas mixture as the feed was introduced and the temperature was increased to the reaction temperature. The effluent gases were analyzed by two gas chromatographs. The hydrocarbon products, including C_2 and condensable C_6–C_{12} aromatics such as benzene,

toluene, xylene and naphthalene, were analyzed by an on-line FID gas chromatograph using a six-way sampling valve heated to 533 K on a Porapak-P column, while H_2, Ar, CO, CH_4 and CO_2 were analyzed by another on-line TCD GC on an activated carbon column, the same as reported elsewhere [19–21]. By using 10% Ar as an internal standard, methane conversion, selectivities towards hydrocarbon products and coke formation were evaluated according to the mass balance of carbon. All reaction rates were based on carbon and expressed as nmol/(g-cat·s).

2.3. Catalyst characterization

Specific surface areas of the samples before and after the dealumination treatment were obtained by the BET method based on adsorption isotherms at liquid nitrogen temperature, and using a value of 0.162 nm^2 for the cross-sectional area of the N_2 molecule. The measurements were performed with Omnisorp 100CX (Beckman Coulter Co.) equipment and the data were processed by a computer.

XRD patterns were obtained on an MPX3 X-ray diffractometer (Mac Sci. Ltd.) using Cu K_α radiation at room temperature and instrumental settings of 40 kV and 100 mA. The powder diffractograms of various samples were recorded from 5° to 50° at a scanning rate of 5°/min. MAS NMR spectra were obtained at 9.4 T on a Bruker DRX-400 spectrometer using 4 mm ZrO_2 rotors. ^{27}Al MAS NMR spectra were recorded at 104.3 MHz using a 0.75 μs ($\pi/12$) pulse with a 2 s recycle delay and 800 scans. A 1% aqueous $Al(H_2O)_6^{3+}$ solution was used as the reference for chemical shifts, and samples were spun at 8 kHz. ^1H MAS NMR spectra were collected at 400.1 MHz using single-pulse experiments with $\pi/2$ pulse and a 4 s recycle delay. All the ^1H spectra were accumulated for 200 scans and spun at 5 kHz. The chemical shifts were referenced to a saturated aqueous solution of sodium 4,4-dimethyl-4-silapentanesulfonate.

NH_3 temperature-programmed desorption (NH_3-TPD) was performed on an AMI1 (Altamira Co.) instrument with a thermal conductivity detector. 0.1 g of the sample was first flushed with He (30 ml/min) at 773 K for 30 min, then cooled to 393 K and saturated with NH_3 until equilibrium. It was then flushed with He again until the baseline of the integrator was stable. NH_3-TPD was then promptly started from 393 to 973 K at 20 K/min. All profiles were deconvoluted into three peaks by the Gaussian curve-fitting method.

The temperature-programmed oxidation (TPO) was carried out on the same AMI1 instrument. In a typical experiment, 10% O_2/He at 15 ml/min was fed into the sample cell under ambient conditions. The temperature was increased linearly at 10 K/min from ambient temperature to 1023 K, at which all the carbon deposit was totally oxidized. The profiles were deconvoluted into two peaks by the Gaussian curve-fitting method.

3. Results and discussion

3.1. Characterization and dealumination of HMCM-22 zeolite

The catalytic dehydrocondensation of methane over Mo catalyst supported on HMCM-22 zeolite was studied as previously reported [17,18,25,26]. The catalytic performance on Mo/HMCM-22 is featured with a higher yield of benzene and a lesser yield of naphthalene in comparison with that on Mo/HZSM-5 catalyst. In addition, it was found that much more coke deposited on Mo/HMCM-22 catalyst, compared with that on conventional Mo/HZSM-5 catalyst [25]. They proposed the catalytic feature on the Mo/HMCM-22 catalyst be mainly related with its unique pore system. The existence of large numbers of 7.1×18.2 Å cavities on HMCM-22 zeolite was attributed to its higher coke deposition than that of HZSM-5 zeolite [25,26]. Although the Mo/HMCM-22 catalyst is a high coking-tolerance catalyst for methane dehydrocondensation, it should be noted that the deposited coke on the catalyst surface is still lowering the selectivity to desired products, poisoning the active center for the catalytic reaction and leading to the deactivation of the catalyst. On considering this, great attention should be paid to the suppression of coke formation on Mo/HMCM-22, in particular from the practical utilization of this catalyst. To achieve this purpose, a dealumination treatment of HMCM-22 zeolite before the catalyst preparation has been conducted and the corresponding results are presented as follows.

3.1.1. Structure characterization by XRD and MAS NMR before and after dealumination

The X-ray diffraction pattern of the HMCM-22 sample shows the same features reported in the patent, both in position and relative intensity of the diffraction peaks [24]. After the dealumination treatment by acid reflux, it was found that both the positions and intensities of the XRD peaks were comparable with those of its corresponding initial zeolite (XRD patterns not shown here). Furthermore, the BET experiment shows that the surface area of the dealuminated HMCM-22 zeolite (510 m^2/g) was also similar to that of the initial HMCM-22 zeolite (521 m^2/g). Accordingly, it suggests that the microporous structure of the HMCM-22 zeolite be retained fully before and after the dealumination treatment.

The ^{27}Al MAS NMR technique is sensitive to variations of zeolitic structure and has been extensively used to discriminate the different states of the aluminum atoms in zeolites, such as framework aluminum atoms in tetrahedral coordination and nonframework aluminum atoms in octahedral coordination [27]. Solid-state ^{27}Al MAS NMR spectra of the parent and dealuminated HMCM-22 zeolites are shown in figure 1(a). For the

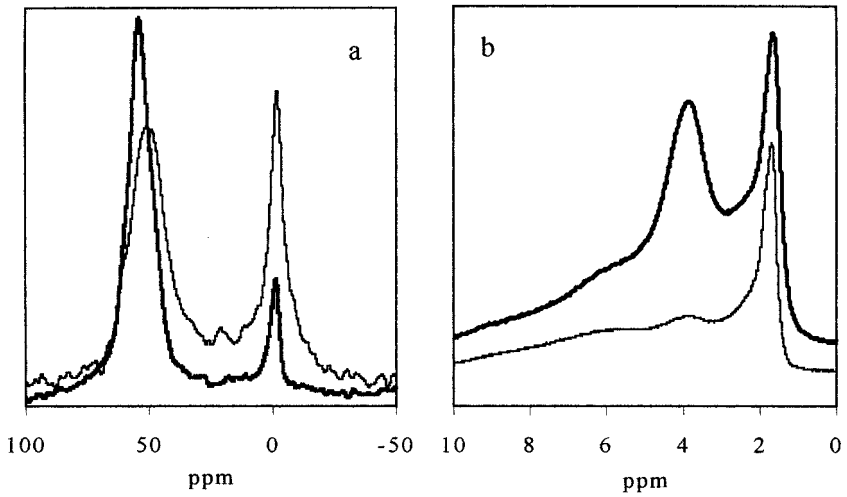

Figure 1. (a) ^{27}Al and (b) ^{1}H MAS NMR spectra of parent HMCM-22 (bold line) and dealuminated HMCM-22 (narrow line), respectively.

parent HMCM-22 zeolite, two distinct peaks with chemical shifts at 0 and 55 ppm are clearly resolved, which are assigned to octahedral extraframework aluminum and tetrahedral framework aluminum, respectively [28,29]. For the dealuminated HMCM-22 zeolite, the intensity of tetrahedral framework aluminum decreased and the overall line width broadened, as compared with that of the parent zeolite. On the contrary, the intensity of extraframework octahedral aluminum at 0 ppm increased greatly. Thus, some of the framework aluminum was really removed from the HMCM-22 zeolite framework after the dealumination treatment.

In addition, we used the solid-state ^{1}H MAS NMR technique to study the variation of zeolite structure before and after the dealumination treatment. The corresponding ^{1}H MAS NMR spectra of the parent and dealuminated HMCM-22 zeolites are shown in figure l(b). There are three peaks centering respectively at about 1.6, 3.7 and 6.0 ppm in the ^{1}H MAS NMR spectrum of the parent HMCM-22 sample. The peak at 1.6 ppm can be attributed to silanol groups, while that at 3.7 ppm can be reasonably assigned to framework Al(Si)-bridging OH groups (Brønsted acid sites) [30–32]. The line at 6.0 ppm can be ascribed to water molecules adsorbed on Lewis sites [33], as well as to a different kind of Brønsted acid sites that interacts electrostatically with the zeolite framework [34,35]. It should be noted that the signal at 3.7 ppm, corresponding to Brønsted acid sites, was drastically suppressed after the dealumination treatment. This again testified to a partial removal of aluminum from the HMCM-22 zeolite framework.

3.1.2. *Acidity of HMCM-22 zeolite before and after dealumination*

Experiments of temperature-programmed desorption of ammonia (NH_3-TPD) were also carried out to study the variation of acidity before and after the dealumination treatment. Figure 2 shows the NH_3-TPD profiles of the parent and dealuminated HMCM-22 zeolites. Meanwhile, their curve-fitting results are listed in table 2. As shown, there are three peaks located at 572,

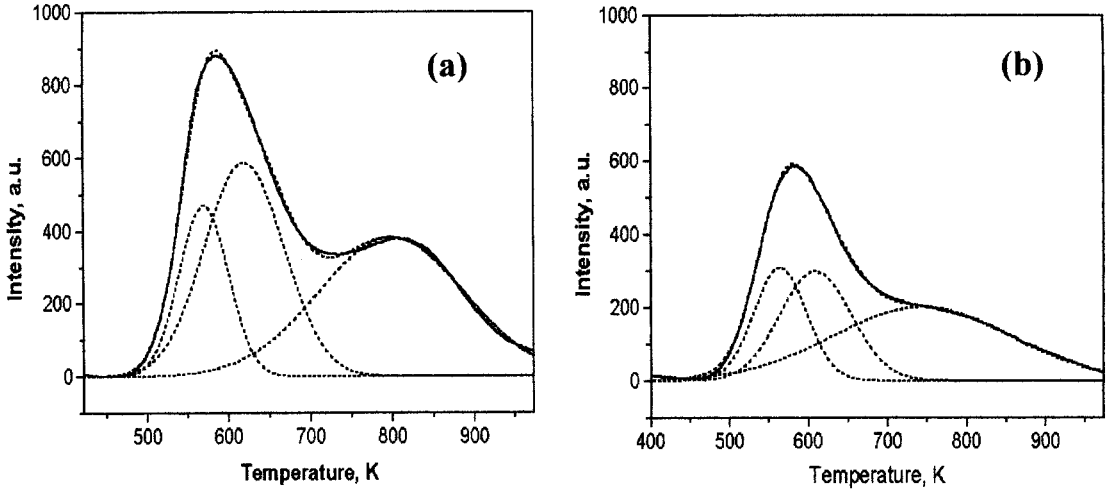

Figure 2. NH_3-TPD profiles of (a) parent HMCM-22 and (b) dealuminated HMCM-22 zeolite. Solid line: experimental value; dash line: calculated value.

Table 2
Peak temperatures of NH_3-TPD profiles and the corresponding amounts of acid sites of parent and dealuminated HMCM-22 zeolites

Sample	Peak (L)		Peak (M)		Peak (H)	
	Temperature (K)	Area (a.u.)	Temperature (K)	Area (a.u.)	Temperature (K)	Area (a.u.)
Parent HMCM-22	572	36 531	622	71 825	804	83 818
Dealuminated HMCM-22	568	26 799	620	34 149	758	56 310

622 and 804 K on the parent HMCM-22 zeolite. The NH_3-TPD results of the HMCM-22 in our experiments are reasonably consistent with the results of the HMCM-22 reported by Unverricht *et al.* [28]. The slight difference in the peak temperatures perhaps resulted from the sample with different SiO_2/Al_2O_3 ratios and from different experimental conditions. As claimed [28], the peak at 572 K was attributed to the desorption of the physisorbed NH_3 species and/or NH_3 adspecies residing on non-exchangeable cationic sites, while the peak at 622 K was assigned to the desorption of NH_3 adspecies adsorbed on exchangeable protonic sites, *i.e.*, Brønsted acid sites. Finally, the peak at 804 K is attributed to strong Lewis acid sites. As can be seen, after the dealumination treatment, all of the areas of peak L, peak M and peak H decreased, but the area of peak M, corresponding to the Brønsted acid sites, decreased drastically, by ~52%. Hence, this further testified to the obvious reduction of Brønsted acid sites owing to the efficient removal of tetrahedral framework aluminum.

3.2. Catalytic performance of modified Mo/HMCM-22 catalyst by the dealumination treatment

3.2.1. Effect of the dealumination treatment

The catalytic performances of Mo supported respectively on dealuminated HMCM-22, initial HMCM-22 and HZSM-5 for methane conversion at 973–1073 K, 3 atm and 2700 ml/(g·h) are listed in table 3. As shown, the catalytic performance on the 6%Mo/HMCM-22 catalyst is featured with a higher yield of benzene and a lower yield of naphthalene as well as more coke deposition, compared with that on the 6%Mo/HZSM-5 catalyst, similar to previous reports [17,18,25,26]. It has also been clearly demonstrated that the dealumination treatment of HMCM-22 zeolite exerted a significant effect on the catalytic performance, as listed in table 3. The lower coke formation and higher benzene formation selectivities were achieved on this modified Mo/HMCM-22 catalyst by the dealumination treatment, compared with unmodified Mo/HMCM-22 catalyst. Specifically, at 973 K, the coke selectivity on the 6%Mo/HMCM-22-D was 22.7%, while that on the 6%Mo/HMCM-22 was 43.4%, almost reduced by half. Furthermore, the benzene selectivity on the former increased from 46.2 to 52.0%. With a further increase of the reaction temperature from 973 to 1073 K, the decreasing trend in coke formation and the opposite trend in benzene formation became more evident. For instance, at 1073 K, benzene selectivities on the 6%Mo/HMCM-22-D, 6%Mo/HMCM-22 and 6%Mo/HZSM-5 were 43.2, 11.7 and 0%, respectively, whereas the coke selectivities were 39.3, 81.1 and 93.4%. Among the tested catalysts, the 6%Mo/HMCM-22-D exhibited a remarkable activity for methane dehydrocondensation, and with a higher selectivity towards benzene and a lower selectivity for coke, particularly for reactions at high temperatures such as 1023–1073 K.

Table 3
Catalytic performances of the Mo-supported HMCM-22 and HZM-5 zeolite catalysts with and without dealumination treatment in methane dehydrocondensation [a]

Catalyst	Temperature (K)	CH_4 conversion (%)	Rate of product formation [nmol/(g-cat·s)]			Selectivity of product (%)		
			C_6H_6	$C_{10}H_8$	Coke	C_6H_6	$C_{10}H_8$	Coke
6%Mo/HMCM-22-D	973	6.5	1085	192	485	52.0	9.0	22.7
6%Mo/HMCM-22	973	7.5	1150	93	1086	46.2	3.7	43.4
6%Mo/HZSM-5	973	6.9	961	301	806	41.8	13.1	35.1
6%Mo/HMCM-22-D	1023	9.4	1540	285	900	48.8	9.0	28.5
6%Mo/HMCM-22	1023	12.0	1640	105	2301	38.5	2.5	53.7
6%Mo/HZSM-5	1023	11.7	1268	287	2091	32.5	7.4	53.5
6%Mo/HMCM-22-D	1073	12.6	1818	249	1657	43.2	5.9	39.3
6%Mo/HMCM-22	1073	14.0	1273	71	3179	11.7	0.9	81.1
6%Mo/HZSM-5	1073	4.2	0	0	1316	0	0	93.4

[a] 3 atm, 2700 ml/(g·h^{-1}), and the data were taken after 240 min time on stream.

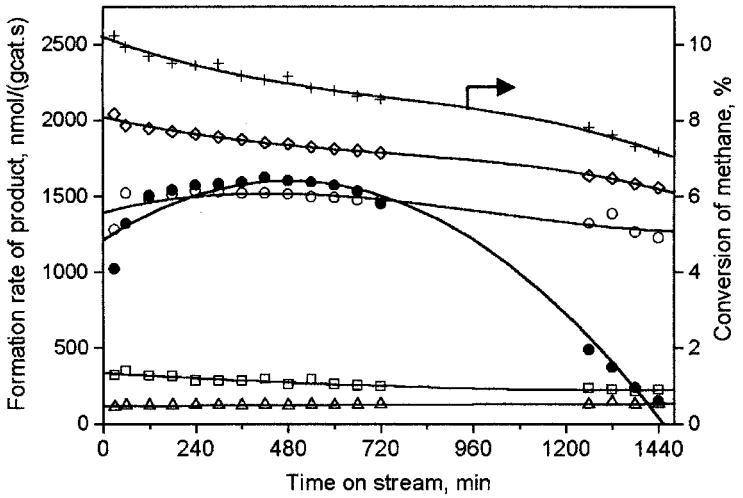

Figure 3. Catalytic performance of 6%Mo/HMCM-22-D at 1023 K, 3 atm and 2700 ml/(g·h) *versus* time on stream in methane dehydrocondensation; +, ○, □, △ and ◇ represent methane conversion, formation rates of benzene, naphthalene, C_2 hydrocarbons and hydrogen (×1/2), separately. Solid circle (●) represents formation rate of benzene on 6%Mo/HMCM-22 under the same reaction conditions.

Figure 3 shows the changes in formation rates of benzene, naphthalene, hydrogen, C_2 hydrocarbons and methane conversion on the 6%Mo/HMCM-22-D catalyst at 1023 K, 3 atm and 2700 ml/(g·h) with on-stream time, in comparison with that of benzene on the 6%Mo/HMCM-22. As presented, the formation rate of benzene (r_{bz}) on both 6%Mo/HMCM-22 and 6%Mo/HMCM-22-D was 1400–1600 nmol/(g-cat·s) in less than 10 h of time on stream. However, r_{bz} on 6%Mo/HMCM-22 decreased drastically after 10 h of time on stream and eventually attained 10% of the initial value. On the contrary, r_{bz} on 6%Mo/HMCM-22-D was quite stable and remained at 85% of its initial value during the prolonged 24 h of time on stream. At the same time, the stable and high hydrogen formation rates of around 4000 nmol/(g-cat·s) were achieved on this 6%Mo/HMCM-22-D catalyst. This high catalytic stability during the methane aromatization reaction under a pure methane feed has never been reported before, especially for the reaction at temperature as high as 1023 K.

3.2.2. *Effect of reaction temperature and CO_2 addition*

Figure 4 presents the catalytic performance of the 6%Mo/HMCM-22-D catalyst by varying the reaction temperature from 973 to 1073 K at 2700 ml/(g·h) and 3 atm. As shown, both the methane conversion (C_{CH_4}) and the benzene formation rate increased greatly at the initial reaction period as the reaction temperature was increased from 973 to 1073 K. Notably, at reaction temperatures between 973 and 1023 K, C_{CH_4} and r_{bz} were quite stable with prolonged time on stream. However, when the reaction temperature was further increased to 1073 K, the activity declined with prolonged reaction time, although a high initial methane conversion of 14% and a high benzene formation rate of 1800 nmol/(g-cat·s) were achieved.

In order to further improve the stability of the catalyst at 1073 K, CO_2 was added to the methane feed. Representative results are shown in figure 5. It is obvious that with the addition of 1.5% CO_2 into the methane

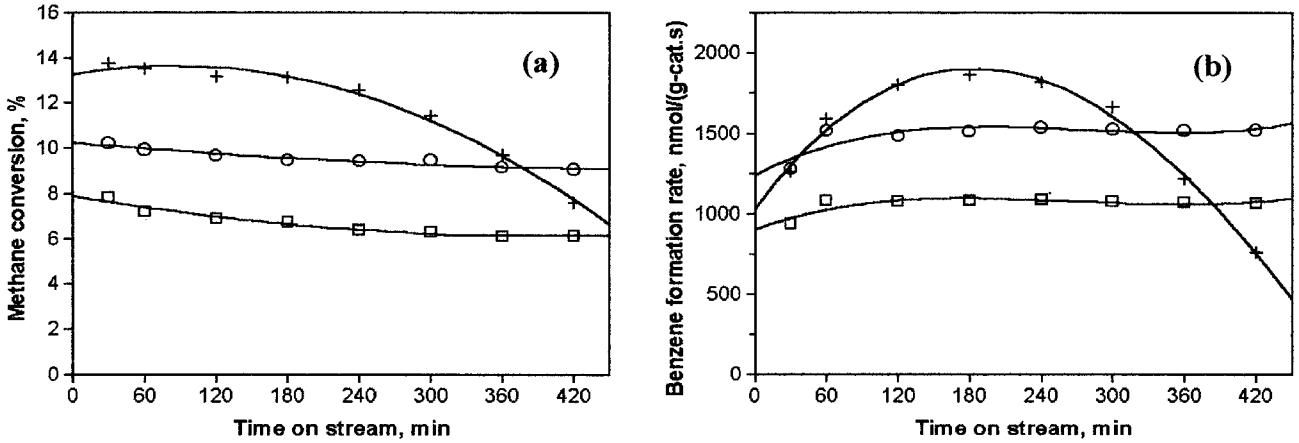

Figure 4. (a) Methane conversion and (b) benzene formation rate of 6%Mo/HMCM-22-D in methane dehydrocondensation at 3 atm and 2700 ml/(g·h) by varying the reaction temperature. □, ○ and + for 973, 1023 and 1073 K, respectively.

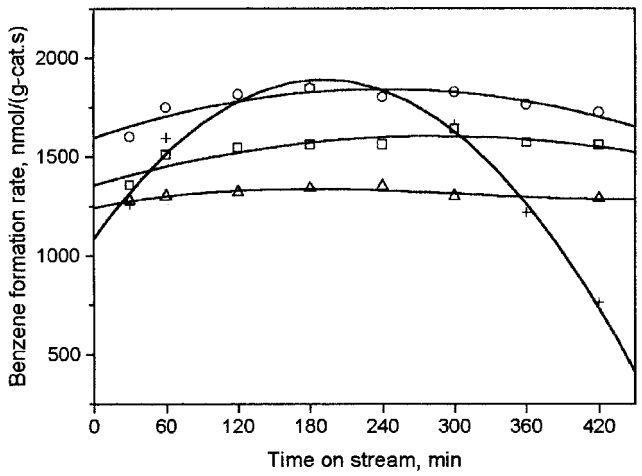

Figure 5. Benzene formation rate of 6%Mo/HMCM-22-D at 1073 K, 3 atm and 2700 ml/(g·h) by varying CO_2%. +, ○, □ and △ for 0, 1.5, 3 and 5 in the feed, respectively.

feed gas, the stability of the 6%Mo/HMCM-22-D catalyst was improved significantly. With a further increase of the CO_2 concentration from 3% to 5%, the stability of the catalyst was further enhanced, but the activity was slightly lowered when compared with the case of adding 1.5% CO_2. A similar promotion effect with the addition of CO/CO_2 to methane feed to stabilize the Mo- and Re-supported HZSM-5 catalysts had been discussed with the effective removal of coke in previous papers [12,19–21]. In this work, the addition of CO_2 to methane feed results in the further improvement of the stability for a modified Mo/HMCM-22 by the dealumination treatment at 1073 K due to the similar mechanism proposed earlier [19,20].

3.2.3. *Effect of catalyst regeneration*

In order to know whether the deactivated 6%Mo/HMCM-22-D catalyst can be regenerated or not by removing the coke, air treatment was carried out on the used catalyst. After treating with flowing air at 823 K for 3 h, the color of the catalyst turned from dark to pure white, and the specific surface area was also restored. Figure 6 shows the reaction results of the fresh and regenerated catalyst at 1023 K, 3 atm and 2700 ml/(g·h). It is evident that both the methane conversion and the formation rate of benzene were completely recovered. The initial r_{bz} on the regenerated catalyst was even slightly higher, *i.e.*, ~200 nmol/(g-cat·s), in comparison with that on the fresh catalyst. But the rate of naphthalene formation on the regenerated catalyst decreased a little, possibly due to the slight narrowing of the channel space [9]. It is interesting to note that the stability of the regenerated catalyst declined slightly, as compared with that of the fresh catalyst. This is probably due to the partial blockage of the zeolite channels and/or loss of Mo species during the course of reaction and regeneration.

3.3. *Characterization of coke by temperature-programmed oxidation (TPO)*

In order to clearly demonstrate the effect of dealumination treatment on the coke formation, TPO experiments of the coked 6%Mo/HMCM-22-D and 6%Mo/HMCM-22 catalysts after reaction at 1023 K for 24 h were conducted and the results are displayed in figure 7. In general, there are two peaks on the recorded profiles. By using a curve-fitting method, the corresponding peak area was estimated

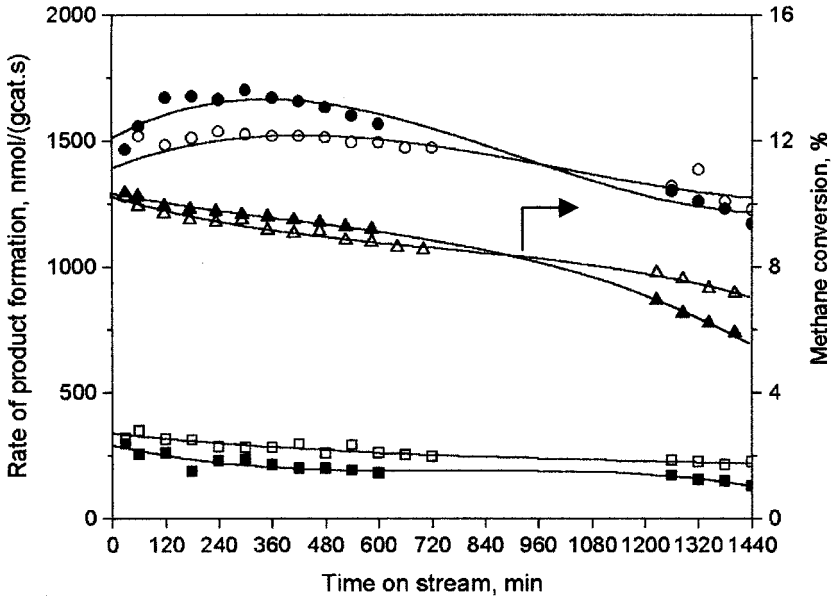

Figure 6. Catalytic performance of fresh (open mark) and regenerated (solid mark) 6%Mo/HMCM-22-D at 1023 K, 3 atm and 2700 ml/(g·h). △, ○ and □ refer to methane conversion and formation rate of benzene and naphthalene, respectively. The regeneration was carried out by air treatment (30 ml/min) at 823 K for 3 h.

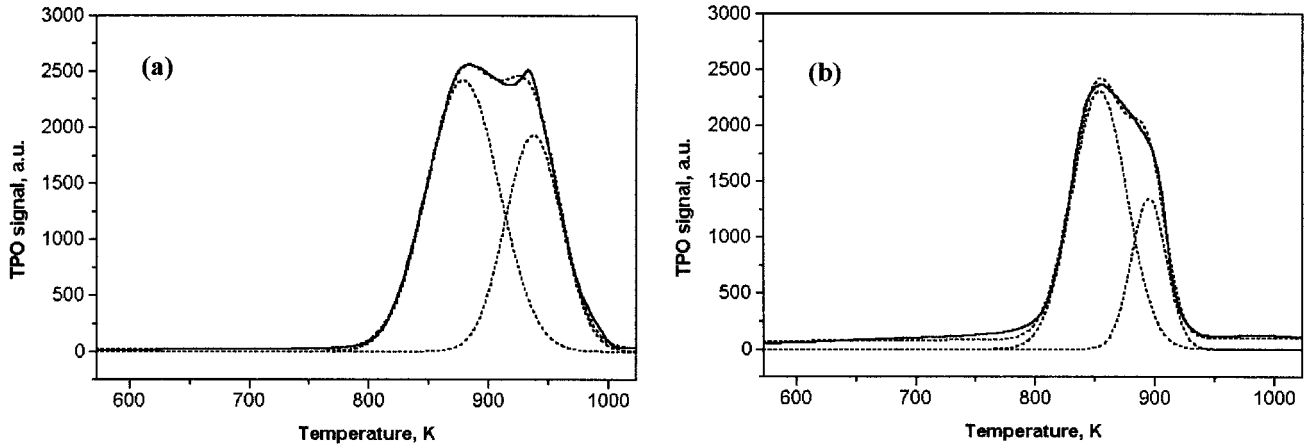

Figure 7. TPO profiles of the coked 6%Mo/HMCM-22 (a) and 6%Mo/HMCM-22-D (b) catalysts after reaction at 1023 K, 3 atm and 2700 ml/(g·h) for 24 h. Solid line: experimental value; dash line: calculated value.

separately, as listed in table 4. The low-temperature peak is at about 878 K and the high-temperature peak is at 937 K for the coked 6%Mo/HMCM-22 catalyst. Referring to previous studies [14,20,36], the low-temperature peak was assigned to carbon related with the Mo species, whereas the high-temperature peak to the carbonaceous deposits on the Brønsted acidic sites of the zeolite support. It is apparent that the coke deposited on the 6%Mo/HMCM-22-D was greatly suppressed as compared with that on the 6%Mo/HMCM-22, particularly for the coke on the zeolite Brønsted acid sites. Specifically, the area of the high-temperature TPO peak on the coked 6%Mo/HMCM-22-D decreased by 56%, while that of the low-temperature TPO peak decreased by 27%, in comparison with those of the coked 6%Mo/HMCM-22. Moreover, the coke formed on the 6%Mo/HMCM-22-D was easier to oxidize than that on the 6%Mo/HMCM-22, as revealed from the lowering of the TPO peak temperature.

3.4. Correlation between the coke formation and zeolite acidity

From the above findings, we can propose the relationship between the coke formation and zeolite acidity. According to the ^{27}Al and ^{1}H MAS NMR spectra (figure 1) and NH_3-TPD results (figure 2), it is obvious that with the distinct removal of tetrahedral Al from the zeolite framework, the Brønsted acid sites of HMCM-22 zeolite decrease. In addition, the reaction results (table 3 and figure 3) and TPO profiles (figure 7) demonstrate the obvious suppression of coke formation, the improvement of benzene selectivity and stability of the modified Mo/HMCM-22 catalyst by the dealumination treatment. These facts indicate that the removal of excess tetrahedral framework Al will inhibit the formation of harmful coke and therefore enhance the benzene selectivity and catalyst stability. It also suggests that only a relatively small amount of Brønsted acid sites is necessary for Mo/HMCM-22 to be an effective methane aromatization catalyst. The excess Brønsted acid sites of the catalyst will benefit the formation of carbonaceous deposits, which will cover the active sites, block the channels and damage the activity of the catalyst.

4. Conclusions

1. The modified Mo/HMCM-22 catalyst by the dealumination treatment exhibited a higher yield and selectivity for benzene production with lower formation of coke in the dehydrocondensation of methane, as compared with those of the unmodified Mo/HMCM-22 catalyst. An excellent catalytic stability along with a high benzene formation rate of 1500 nmol/(g-cat·s) was achieved on 6%Mo/HMCM-22-D catalyst at

Table 4
Peak temperatures of TPO profiles and the corresponding amounts of coke on the used 6%Mo/HMCM-22 and 6%Mo/HMCM-22-D catalysts after reaction at 1023 K for 24 h

Sample	Peak (L)		Peak (H)	
	Peak temperature (K)	Area (arbitrary units)	Peak temperature (K)	Area (arbitrary units)
6%Mo/HMCM-22	878	183 293	937	113 424
6%Mo/HMCM-22-D	852	133 804	895	49 366

1023 K during the prolonged 24 h of time on stream, owing to the distinct suppression of coke formation.
2. XRD and BET measurements provided evidence that the microporous structure and the zeolite framework of HMCM-22 zeolite was unchanged before and after the dealumination treatment by aqueous HNO_3 solution.
3. Solid-state ^{27}Al and ^{1}H MAS NMR experiments showed a partial removal of tetrahedral aluminum from the HMCM-22 zeolite framework and a distinct decrease of Brønsted acid sites (proton form in Al–O–Si) after the dealumination treatment, which was consistent with the results attained by NH_3-TPD study.
4. The remarkable suppression of coke formation on the modified Mo/HMCM-22 catalyst by the dealumination treatment is related to an effective decrease of strong acid sites, particularly of the strong Brønsted acid sites.

Acknowledgments

This work was supported by the New Energy and Industrial Technology Development Organization (NEDO) of Japan. The authors thank Professors Xinhe Bao, Xiuwen Han, Yide Xu and Longya Xu of the Dalian Institute of Chemical Physics for their kind help in NMR experiments and for the provision of the HMCM-22 zeolite.

References

[1] R.H. Crabtree, Chem. Rev. 95 (1995) 987.
[2] Y. Xu and L. Lin, Appl. Catal. A 188 (1999) 53.
[3] L. Wang, L. Tao, M. Xie, G. Xu, J. Huang and Y. Xu, Catal. Lett. 21 (1993) 35.
[4] Y. Xu, S. Liu, L. Wang, M. Xie and X. Guo, Catal. Lett. 30 (1995) 135.
[5] L. Chen, L. Lin, Z. Xu, X. Li and T. Zhang, J. Catal. 157 (1995) 190.
[6] F. Solymosi, A. Erdohelyi and A. Szoke, Catal. Lett. 32 (1995) 43.
[7] F. Solymosi, A. Szoke and J. Cserenyi, Appl. Catal. A 142 (1996) 361.
[8] D. Wang, J.H. Lunsford and M.P. Rosynek, Topics Catal. 3 (1996) 289.
[9] D. Wang, J.H. Lunsford and M.P. Rosynek, J. Catal. 169 (1997) 347.
[10] S. Liu, Q. Dong, R. Ohnishi and M. Ichikawa, Chem. Commun. (1997) 1445.
[11] S. Liu, L.Wang, R. Ohnishi and M. Ichikawa, J. Catal. 181 (1999) 175.
[12] L. Wang, R. Ohnishi and M. Ichikawa, Catal. Lett. 62 (1999) 29.
[13] R.W. Borry III, Y.H. Kim, A. Huffsmith, L.A. Reimer and E. Iglesia, J. Phys. Chem. B 103 (1999) 5787.
[14] W. Ding, S. Li, G.D. Meitzner and E. Iglesia, J. Phys. Chem. B 105 (2001) 506.
[15] Y. Lu, Z. Xu, Z. Tian, T. Zhang and L. Lin, Catal. Lett. 62 (1999) 215.
[16] Y. Shu, D. Ma, X. Bao and Y. Xu, Catal. Lett. 66 (2000) 161.
[17] Y. Shu, D. Ma, L. Xu, Y. Xu and X. Bao, Catal. Lett. 70 (2000) 67.
[18] Y. Shu, D. Ma, L. Su, L. Xu, Y. Xu and X. Bao, Stud. Surf. Sci. Catal. 136 (2001) 27.
[19] S. Liu, L. Wang, Q. Dong, R. Ohnishi and M. Ichikawa, Chem. Commun. (1998) 1217.
[20] R. Ohnishi, S. Liu, Q. Dong, L. Wang and M. Ichikawa, J. Catal. 182 (1999) 92.
[21] L. Wang, R. Ohnishi and M. Ichikawa, J. Catal. 190 (2000) 276.
[22] Y. Lu, D. Ma, Z. Xu, Z. Tian, X. Bao and L. Lin, Chem. Commun. (2001) 2048.
[23] P. Wu, T. Komatsu and T. Yashima, Micropor. Mesopor. Mater. 22 (1998) 343.
[24] M.K. Rubin and P. Chu, US Patent 4,954,325 (1990).
[25] Y. Shu, R. Ohnishi, M. Ichikawa, D. Ma, L. Xu, Y. Xu and X. Bao, Catalysts & Catalysis 43(2) (2001) 137.
[26] Y. Shu and M. Ichikawa, Catal. Today 71 (2001) 55.
[27] A.T. Bell and A. Pines, *NMR Techniques in Catalysis* (Marcel Dekker, New York, 1994).
[28] S. Unverricht, M. Hunger, S. Ernst, H.G. Karge and J. Weitkamp, Stud. Surf. Sci. Catal. 84 (1994) 37.
[29] D. Ma, Y. Shu, X. Han, X. Liu, Y. Xu and X. Bao, J. Phys. Chem. B 105 (2001) 1786.
[30] M. Hunger, Catal. Rev. Sci. Eng. 39 (1997) 345.
[31] M. Muller, G. Harvey and R. Prins, Micropor. Mesopor. Mater. 34 (2000) 281.
[32] Y. Shu, D. Ma, X. Liu, X. Han, Y. Xu and X. Bao, J. Phys. Chem. B 104 (2000) 8245.
[33] M. Hunger, D. Freude and H. Pfeifer, J. Chem. Soc., Faraday Trans. 87 (1991) 657.
[34] E. Brunner, K. Beck, L. Heeribout and H.G. Karge, Micropor. Mater. 3 (1995) 395.
[35] L.W. Beck and J.F. Haw, J. Phys. Chem. 99 (1995) 1076.
[36] H. Jiang, L. Wang, W. Cui and Y. Xu, Catal. Lett. 57 (1999) 95.